Radiometric dating (U/Th) of the lower marine terrace (Tyrrhenian, MIS 5.5) west of Nice (French Riviera). Morphological and neotectonic quantitative implications.

Michel Dubar[a*], Christophe Innocent[b] and Olivier Sivan[c].

[a] CNRS, Cepam – UMR 6130 250 rue Albert-Einstein 06560 Valbonne
[b] BRGM, 3 avenue Claude Guillemin 45060 Orléans, cedex2
[c] INRAP, 24 avenue de la Grande Bégude, 13770 Venelles

Mots-clés : datations U/Th, coquilles, terrasses marines, stade isotopique 5.5, néotectonique, littoral ligure, arc de Nice
Keywords : U/Th datations, shells, marine terrace, MIS 5.5, neotectonic, French Riviera, Nice range.

I. Introduction.

Morphologically, the Quaternary terraces in the area of Nice consist of eight stepped levels, over height of 100 m. This morphology is the result of a tectonic uplift of the coast combined with glacio-eustatic quaternary changes in sea-level. Each terrace level corresponds to an interglacial highstand in sea-level and each thus-determined perfectly horizontal line may thus serve as a morphological guide-mark in order to detect deformations of the coast
In the Nice area where active seismicity and neotectonics are well documented [4], we focused more specifically on a survey of the lower, most recent, terrace with the aim of detecting and quantifying all possible deformations. This has entailed concentrated on the longest profile of the lower terrace along the coast, starting from the Provencal foreland, west of Nice, and running eastward in front of the Nice Alpine range (Fig.1). In practice, the new dates obtained west of Nice are compared with earlier palaeontological data obtained from further east, in an attempt to connect the lower terraces of the two sectors.

II. The Tyrrhenian terrace : context and previous work

The eight Quaternary terraces are stepped below the Pliocene delta of the River Var [21]. The highest (and oldest), around 110 m a.s.l., was dated by a foraminiferal assemblage to the Calabrian period (1,7-1,4 Ma). The lowest should be dated to the Tyrrhenian highstand (last interglacial period, MIS 5). Indeed, the presence of *Strombus bubonius* on the Nice coast undoubtely links it to the Mediterranean Basin Tyrrhenian Age [35]. However, this species is not common west of Nice; it was found at only one spot [23]. Thus the lower marine terrace remains to this day badly dated. More recently [11], we have pointed out the presence of a typical terrestrial malacofauna in the dune deposits of the lower coastal terrace. This land

* Corresponding author dubar@cepam.cnrs.fr

snail assemblage includes several extinct or exotic species living today in the Apennine area. In the Nice area and on the French Riviera this fauna was encountered only on the lower terrace and is thus a good marker. Detailed stratigraphic analysis emphasises a climatic evolution of clear interglacial type, correlated with stage 5 of the Western Mediterranean Basin [11]. In view of recent improvements in radiometric technology and methods, we have attempted to date this malacofauna and thus verify the above results.

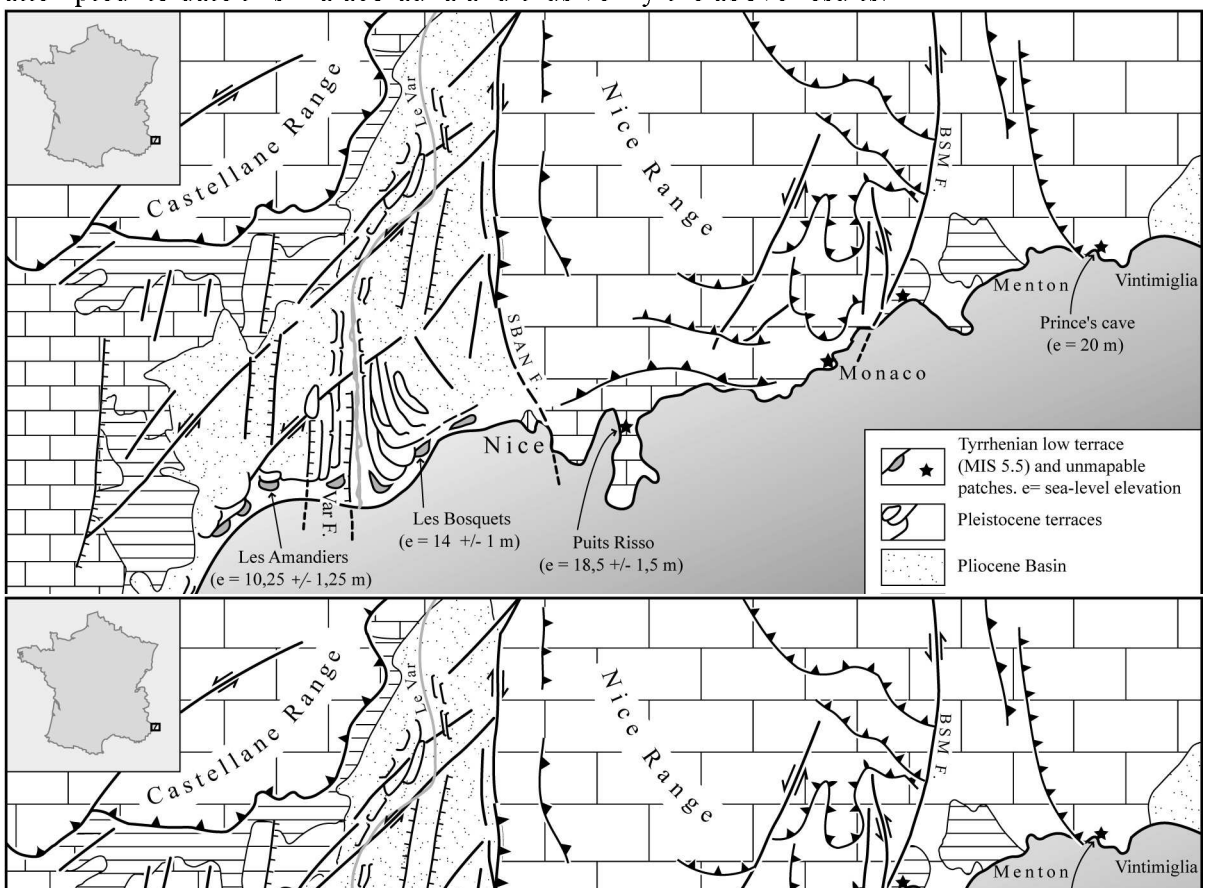

Fig. 1. Geomorphological and structural framework of the Southern Alps and French Riviera between Antibes and Vintimiglia. Tyrrhenian Sea-level values (e) are explained in the text. The structural features of the Var Basin are from Guglielmi (1993). SBAN F.: Saint-Blaise-Aspremont-Nice Fault; BSM F. : Breuil-Sospel-Monaco Fault.

Schéma géomorphologique et structural des Alpes-Maritimes entre Antibes et Vintimille. Les valeurs du niveau marin (e) sont expliquées dans le texte. Les structures tectoniques du bassin du Var sont d'après Gugliemi et Dubar,1993 [15]. SBAN F.: accident Saint-Blaise-Aspremont-Nice : BSM F. : accident Breuil-Sospel-Monaco

III. Method to determine ancient sea-levels

In order to relate sea-level to the sediments under examination, specific sedimentological or geomorphological indicators known from present beaches or nearshore profiles of the region were made use of. Present profiles were recorded at various points according to the nature of the substratum and to the morphology of the coast.

Past relative sea-level is shown through some sedimentological indicators by comparing them with present beaches or nearshore profiles. Profiles were chosen from different sectors according to geomorphological features of the coast.

The above-mentionned heights take into account the mean value of tide, that is 30 cm in this part of the Mediterranean Basin.

West of Nice, the littoral is sandy-gravelly with shallow beach-profiles, poor in sediment [30]. From nearshore to backshore, the sequence layers is as follow : sand or terrigenous sand, gravels calibrated around the 1,25 mm median value and flattened pebbles. The limit between sand and gravels is located around -1,5 m [25]. The transition from gravels to flat pebbles takes place between the hydrographic zero and +1m. Behind the berm, crest and other scarps, pebbles form a barrier which reaches up to an altitude of 3 m, regarless of the length and slope of the barrier.

East of Nice, the rocky and scarped coast accomodates only small beaches. Profiles are short and steep, and reach down submarine steps in a still wave-dominated environment. Sands are abundant only in sectors where fluvial supplies from tertiary basins are important, as in the Bays of Menton or Vintimiglia. Generally, beaches are skeletal and consist solely of blocks. Storms frequently perturb the beach system and determine the formation of shingle bars, several meters above sea-level, but these do not last and are dismantled. Thus, the normal backshore lies generally placed between 2.5 and 3 m above sea-level.

Of course these elements organised according to their profiles may exhibit some perturbations depending on waves and currents conditions : infratidal sands, backswash gravels and surf pebbles may mix. In that case, the error bar on sea-level will be increased (3+1,5 = 4,5 m. for the maximum). In the best of cases, the error bar will be reduced to the strict extension margin of the observed element.

Sedimentary facies	**West of Nice**	**East of Nice**
Sand	<-1,5 m	-
Gravels	-1,5 à +1 m	-
Pebbles	+1 à +3 m	-
Mixed	-	infralittoral -10 m to +3 m

Table. 1 – Estimation of the altimetric distribution of beach sediments
Distribution altimétrique des sédiments de plage

IV. Sites studied for dating and geomorphological setting of the low marine terrace, west of Nice.

In a recent survey aiming to revise the geological map of Grasse-Cannes [10], the Quaternary terraces situated west of Nice were the subject of a detailed cartographic study at 1/25 000. Other detailed investigations were carried out by INRAP in the course of urban development in Nice-City.

From Antibes to Nice, Quaternary marine terraces broadly expand according to the width ot the coastal plain. The Pliocene delta deposits of the Var Basin have embedded

themselves into Provence Mezozoic limestones. Although this is a low-flat shore, as one approaches the Alpine reliefs, one observes a progressive increase in topography. The lower terrace, which is a few meters above the coastal plain, can be closely observed along the coast, west and east of the mouth of the Var. Both sites studied belong to each of these sectors.

Measurements of altitude were taken with an electronic altimeter (accuracy : 0,50 m) calibrated on the hydrographic zero.

1. Les Amandiers (Cros-de-Cagnes ; x= 7°09'18'' y= 43°39'31'' z= 10 m)

West of the mouth of the Var river, the lower terrace is represented by wide benches located around 10 m in altitude (Fig. 1). Near Cros-de-Cagnes a cross-section shows marine gravels of the nearshore facies (Table 1) situated at 10 m a.s.l. which indicate sea-level between 9 and 11,5 m (10,25 ± 1,25 m). Marine deposits are associated with strong lagunal clays and dune sands which lay backbeach. Further inland, on the first slopes, they interstratify with palaeosoils. These deposits contain rich landsnail malacofauna with *Retinella. herculeus* and other species of the Tyrrhenian « ligurian fauna » [11].

2. Les Bosquets (Nice ; x=7°13'48''y= 43°40'57''z=16m)

East of the mouth of the River Var, the lower marine terrace forms a straight bench along the littoral (Fig.1). Marine sands and gravels deposit are exposed between 13 and 16 m in altitude, 6° south. These deposits are typical of the swash zone, very close to zero in sea-level. By using the present beach parameters (Table 1), we can judge the past sea-level to have been between 13 and 15 m (14 ± 1m) in altitude. Some shells of *Ostreidae* have been collected in these deposits. A cross-section perpendicular to the shore evidences landward lagunal and dune deposits and a forest palaeosoil which provided various examples of vertebrate fauna and the so-called « Ligurian landsnail fauna ».

These new data on the lower terrace in this sector corroborate local ancient observations [7] of Tyrrhenian pebbles and blocks and fauna deposits around 11 m in altitude. Nevertheless, the exact position of the sea-level cannot be restored.

West of Les Bosquets, near the Saint-Augustin railway station, a pebble bench lying around 15 m a.s.l. is another marker for the Tyrrhenian terrace.

Both sites were dated on the basis of shells, the former thanks to the landsnail species *R. herculeus*, the latter to one sea shell *O. lamellosa.*

V. U/Th dating

1. Analytical techniques

U-Th analyses have been carried out on four total shells of *R. herculeus* from Cros de Cagnes, and on six fragments of a single valve of *O. lamellosa* from the Les Bosquets site. Procedures of cleaning and of U-Th chemical separation have been described by Innocent *et al.* [20].

U and Th were measured on a MC-ICP-MS "Neptune" mass spectrometer equipped with an "Apex®" desolvator and an ion counter coupled with a "RPQ" filter. Samples were corrected, using the standard bracketing method, for a global measurement bias factor encompassing the mass fractionation and the yield of the ion counter. Such correction allows

one to dispose of sharp variations of the yield that may occur between the time of external calibration and the time of sample measurement. Moreover, this correction is justified by the fact that mass fractionation effects are reliably described using a linear law [34], considering the uncertainty levels typical of U-Th measurements. Ion beams measured by the ion counter ranged as possible between 1 and 4 10^4 coups per second to avoid the bias effect that could possibly result from an unadequate dead time correction and also for the ion beam intensity to be sufficient enough to minimize as possible internal uncertainties.

For U, the certified reference material (CRM) U010 standard was used. 235 and 238 peaks were measured on a Faraday cup, and 234 on the ion counter. For Th, the CRM IRMM 035 standard was used, plus two additional standard solutions that have been synthetized at BRGM Orléans : Th 103 and Th 104 [19]. Both solutions, though not certified as reference materials, have isotopic compositions that are closer than CRM IRMM 035 to those measured in the shells. Thus, CRM IRMM 035 was used in addition to Th 103 and Th 104 solutions for standard bracketing during analysis sequences. For U and Th concentration measurements, artificial isotopes (^{233}U, ^{236}U, ^{229}Th) were all measured on a Faraday cup. In order to evaluate the Th mass fractionation *sensu stricto* and its drift through time, the Th 103 standard was measured at the beginning and at the end of each Th sequence, using a Th 103 solution sufficiently concentrated for ^{230}Th to be measured on a Faraday cup.
Total blanks were lower than 70 pg for U and 200 pg for Th. Results are reported in Table 2.

Echantillon	U (ppm)	Th (ppb)	(^{234}U/^{238}U)	(^{238}U/^{232}Th)	(^{230}Th/^{232}Th)	(^{230}Th/^{238}U)	(^{234}U/^{232}Th)	(^{230}Th/^{234}U)
Os 1	0.720 (03)	1036 (2)	1.1961 (23)	2.162 (10)	3.000 (12)	1.3877 (83)	2.586 (13)	1.1602 (73)
Os 2	1.380 (03)	866 (1)	1.1797 (19)	4.959 (14)	6.399 (31)	1.2905 (72)	5.850 (19)	1.0939 (64)
Os 3	2.774 (09)	801 (5)	1.1646 (46)	10.783 (78)	13.222 (57)	1.2262 (103)	12.557 (103)	1.0529 (98)
Os 4	1.206 (07)	513 (1)	1.1893 (34)	7.314 (41)	9.389 (43)	1.2836 (93)	8.699 (55)	1.0792 (84)
Os 5	1.930 (07)	526 (1)	1.1268 (23)	11.431 (47)	13.526 (53)	1.1833 (68)	12.880 (60)	1.0501 (64)
Os 6	3.456 (11)	317 (1)	1.1233 (26)	33.92 (14)	39.27 (20)	1.1577 (75)	38.100 (177)	1.0306 (71)
Sp 1	0.935 (02)	136.0 (2)	1.6273 (35)	21.41 (07)	27.29 (10)	1.2749 (62)	34.838 (131)	0.7834 (42)
Sp 2	1.521 (03)	50.1 (3)	1.6127 (47)	94.61 (55)	147.27 (58)	1.5566 (110)	152.58 (1.00)	0.9652 (74)
Sp 3	1.555 (06)	57.4 (5)	1.6264 (33)	84.34 (81)	104.30 (64)	1.2367 (142)	137.17 (1.35)	0.7604 (88)
Sp 4	1.549 (07)	99.1 (3)	1.6088 (43)	48.68 (25)	59.39 (28)	1.2200 (86)	78.31 (46)	0.7583 (57)

Table 2. Concentrations and activity ratios measured on *Ostrea* (Os) and *Retinella* (Sp) shells. Uncertainties on the last digits are given as 2σ.
Concentrations et rapports d'activité mesurés sur les coquilles d'Ostrea (Os) et Retinella (Sp). Les incertitudes sur les dernières décimales sont données en double écart-type.

2. Results and discussion

.2.1. *Retinella herculeus*

Three of the four shells define straight lines on ^{238}U/^{232}Th – ^{230}Th/^{232}Th and ^{234}U/^{232}Th – ^{230}Th/^{232}Th diagrams [29] (Fig. 2). There is no clear explanation for the fact that the fourth point plots out of the lines. However, ages can still be calculated : 131 ± 1 ky derived from ^{238}U and 132 ± 2 ky from ^{234}U. These ages are identical and are supposed to date the end of the early U trapping, a few thousand years later than the death of the mollusc [17]. The shells would be thus a few ky older than the Eemian *sensu stricto* [31]. ^{234}U/^{238}U activity ratios are comparable from one shell to another (Table 2). The average initial recalculated ratio is 1.9, clearly higher than the seawater value [16]. This highly ^{234}U-enriched uranium very probably indicates groundwater circulation [27]. Recalculated initial ^{230}Th/^{232}Th activity ratios are 4

("234" diagram) and 4.4 ("238" diagram), much higher than the upper continental crust average value (featuring a secular equilibrium of the ^{238}U decay chain and an elemental Th/U ratio close to 4)

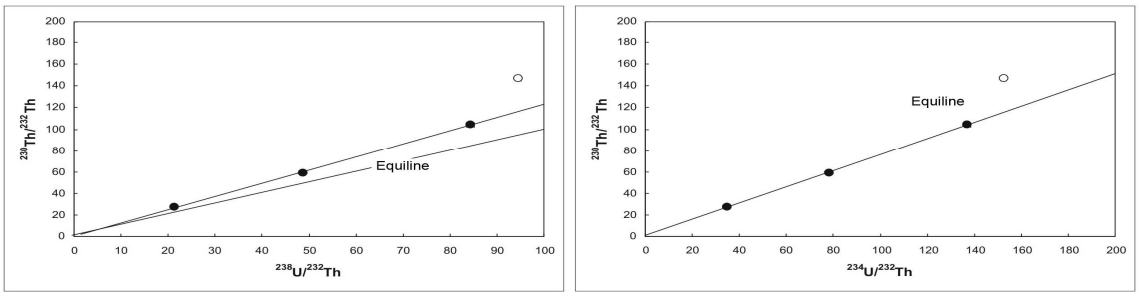

Fig. 2. "Rosholt" U-Th isochron diagrams for the four analyzed shells. The sample that plots out of the isochron is represented as a white disk. Linear regression calculations have been done after [23]. MSWD are of 14 for the "238" isochron and 3 for the "234" isochron.
Diagrammes isochrones U-Th au sens de Rosholt pour les quatre coquilles analysées. L'échantillon qui s'écarte de l'isochrone est représenté en blanc. Les calculs de régression linéaire ont été effectués d'après la méthode de Minster et al. (1979). Les MSWD témoignant de la qualité des alignements sont de 14 pour l'isochrone "238" et de 3 pour l'isochrone "234".

Since one of the four points does not plot on the isochron, it is necessary to test the validity of the age using another type of diagram : $^{232}Th/^{234}U$ – $^{230}Th/^{234}U$ [26]. In this latter diagram (not shown here), the three points still define a straight line, the intercept at X = 0 giving an age that is slightly older, close to 150 ky. Such an age can be considered as too old, as ^{230}Th was present in the shells at the initial time. Thus, the age at 131 – 132 ky seems to be reliable, although derived from only three points.

.2.2. *Ostrea lamellosa*

The six fragments, reported in the Rosholt isochron diagrams (not shown) show alignments that however do not allow to calculate any age, as the datapoints fall above the equiline in both diagrams. The data can be explained by an open-system evolution model (Fig. 3). The shell, containing initially some detrital U and Th, would have trapped marine uranium 130 ky ago. Then, ^{234}U-enriched uranium would have been trapped, resulting from groundwater circulation, with a concomitant leaching of the U present in the shell. The parameters of the evolution model are given in the caption of Fig. 3. This model allows one to explain the measured activity ratios, except for one point for which the initial detrital component was probably higher than for the five other points (Fig. 3).

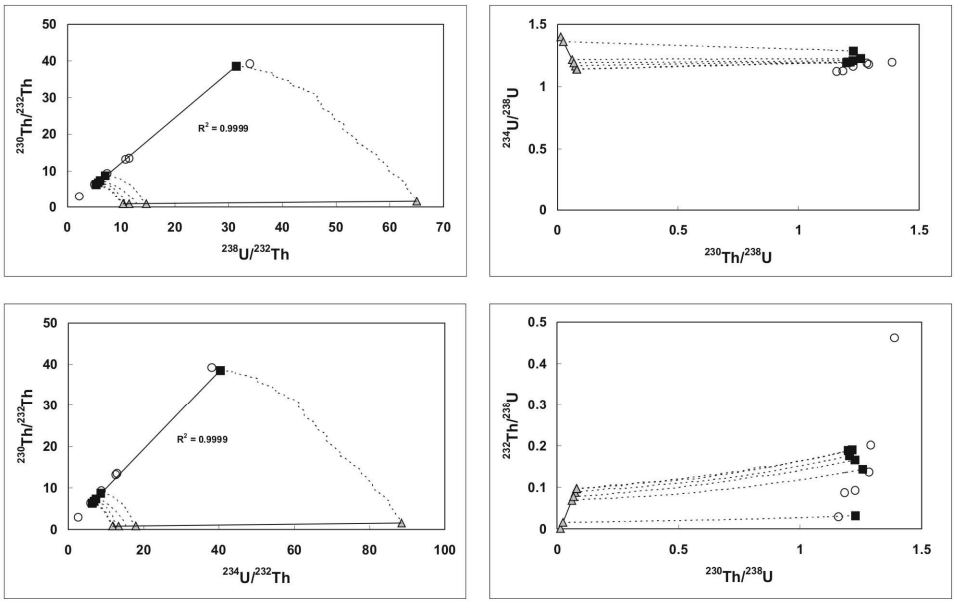

Fig. 3. U-Th diagrams normalized to ^{232}Th (left panel) and ^{238}U (right panel). White disks : measured data; grey triangles : modelized initial points; black squares : present-day, modelized points. The contribution of the initial detrital component is estimated at 7%, the decay chain is at the equilibrium and the elemental Th/U ratio is that of the average upper continental crust (~ 4). The two "water" components are Th-depleted : $^{230}Th/^{234}U = 0.01$. The seawater component is slightly "enriched" in ^{230}Th ($^{230}Th/^{232}Th = 1.15$). The groundwater component is highly "enriched" in ^{230}Th ($^{230}Th/^{232}Th = 14$). The seawater $^{234}U/^{238}U$ activity ratio is 1.148. The groundwater $^{234}U/^{238}U$ activity ratio is 1.4. Gain and/or loss percentages in U and/or Th (by thousand of years and relative to the total amount of element present at a given time) are selected randomly by the computer, between 0 and the chosen upper limit. These are respectively (per ky) : 7.7‰ for U gain, 1.7% for U loss, and 0.77‰ for Th (there is no Th loss). This open-system evolution tends to preserve the alignments in Rosholt isochron diagrams [17] (left panel).
Diagrammes U-Th normalisés à ^{232}Th (gauche) et ^{238}U (droite). Disques blancs; données mesurées; Triangles gris points initiaux modélisés; Carrés noirs : points actuels modélisés. La contribution du composant détritique initial est estimée à 7%, la chaîne est à l'équilibre, avec un rapport Th/U typique de la croûte continentale moyenne supérieure (~ 4). Les deux composants "eau" sont très pauvres en Th : $^{230}Th/^{234}U = 0.01$. Le composant marin est très légèrement "enrichi" en ^{230}Th ($^{230}Th/^{232}Th = 1.15$). Le composant "eau souterraine" est très enrichi en ^{230}Th ($^{230}Th/^{232}Th = 14$). Le rapport d'activité $^{234}U/^{238}U$ du composant marin est de 1.148. Le rapport $^{234}U/^{238}U$ du composant "eau souterraine" est de 1.4. Les termes de perte et gain en U et Th (par millénaire et par rapport à la quantité d'élément présent un instant donné) sont choisis aléatoirement par l'ordinateur entre 0 et la borne supérieure. Ces dernières sont: 7.7‰ pour le gain en U, 1.7% pour la perte, et 0.77‰ pour le gain en Th (il n'y a pas de perte). Ce modèle d'évolution en système ouvert tend à conserver les alignements dans les diagrammes isochrone au sens de Rosholt [18](fig. de gauche).

Thus, the data obtained on the bivalve shell remain compatible with a Tyrrhenian age. However, it appears that a U-series dating study has to involve preferably several single, complete shells. Moreover, gastropods seem definitely to be more reliable than bivalves for such a type of study, in agreement with previously published works [17] [22] [9].

VI. Morpho- Neotectonic implications.

Both U/Th dates and palaeoclimatic data date the lower marine terrace of the western Nice area to the last interglacial highstand (MIS 5.5). A continuity is thus possible on a same profile between the Tyrrhenian deposits west of Nice to those to the east which provided *S.*

bubonius. Such a profile, extends for close to 70 km on either side of the main structural zone which separates the Provence foreland from the Alpine range of Nice. Its morphology and tectonics are analysed for both sectors taking into account old and new data.

1/ Morphology

The sectors situated on either side of Nice offer different morphological features : to the west, the littoral is low and flat along the Provence platform and Pliocene Var Basin; to the east, along the Alpine range, the coast is rocky, scarped and often bordered with calcareous cliffs.

In the first sector, terraces extend widely and exhibit a good continuity. Tyrrhenian deposits lie some ten meters west of the Var, around 16 m to the east of the river mouths. The Tyrrhenian sea-level, restored using sedimentological criteria (table 1), lies around 10 m (10,25 ± 1,25 m) a.s.l. to the west, and around 14 m (14 ± 1 m) to the east (§ IV and Fig.1).

In the second sector, the terraces which are preserved along the coast are reduced to patches of sediments, no more than a few m^2 wide. Nevertheless, patches of Tyrrhenian Age are numerous and rich in fossils including the typical species *S. bubonius*. Numerous radiometric datings were carried out earlier, but the results were partly controversial [14]. Most of the patches under consideration are submarine deposits and their bathymetry is not precisely defined. Thus, the exact position of the Tyrrhenian shoreline is still debated. By referring to reliable markers along the coast (beach sediments and wave notches), the Tyrrhenian shoreline seems to be situated around 20 m in altitude. This is true for « Puits Risso » on the Villefranche peninsula (fig. 1), which provided a rich malacofauna including *S. bubonius* [7] with a restored sea-level, taking into account the error bar (Table 1), between 17 and 20 m (18,5 ± 1,5 m). This position of the sea-level is confirmed in the Prince's cave : the Tyrrhenian series stretches from sands with *S. bubonius* around 12,50 m a.s.l. to a spectacular notch culminating at 22,70 m [1]. Thus the maximum reached in sea-level is close to 20,20 m (estimating the mean sea-level 2,50 m under the notch, according to modern observations). Along the coast, from Nice to Vintimiglia, the other deposits with *S. bubonius* (Fig. 1) around 10-12 m a.s.l. are shown to have been under sea-level. Thus, the Tyrrhenian shoreline must be located around 20 m, maximum elevation of *S. bubonius* deposits. The error bar being 3 m (table 1), we may specify that the relative Tyrrhenian sea-level position was between 17 and 20 m in this sector.

2/ Neotectonics

The complete profile of the lower terrace between Antibes and Vintimiglia exhibits a progressive uplift from west to east [Fig.4] that is consistent with ancient data [6], and correlated with tectonics. Today we may calibrate this uplift and analyse it according data on major regional structures : to the west, the Var fault or rift, located under the Pliocene Basin ; to the east, the fault edges the Nice Alpine range (St-Blaise, Aspremont- Nice Fault, SBAN Fault, Fig.1).

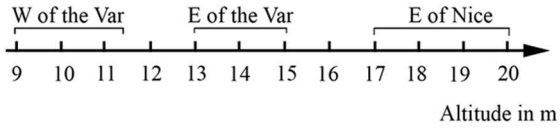

Fig.4. Altimetric position with error bars of the restored Tyrrhenian sea-level in three sectors of the coast.
Altimétrie du niveau marin avec ses marges d'erreur au Tyrrhénien reconstitué dans le divers secteurs côtiers.

The first fault determines an eastern uplift of the lower terrace from 1,5 to 6 m (Tabl.3), taking into account the error-bar (Table 1). This difference in level may be compared with that separating the two banks of the lower River Var and affecting the Pliocene deposits [21] and all the Quaternary terraces [13] [12]. This difference is related to a supposed rift called "Accident du Var" under the Pliocene basin or at least related to a non-homogenous deformation of the basin, constrained by the adjacent active Alpine range border (Fig.1). Under the Pliocene deposits, the mesozoïc limestones are affected by a multiple fault system (N 40 to NS) . This system separates blocks, faulting and uplifting them like the keys of a piano. The vertical throw seems to be at its maximum along a fault just situated in the axis of the present lower Var valley, this leading one to accept the reality of the "Accident du Var " (Fig.1). The neotectonic activity is due to the uplift of the Alpine Nice range. It was paroxysmic during the Upper Pliocene, but remained important during the Pleistocene, so that all the terraces (8 levels) were displaced in level from one bank to the other. The eastern bank is overelevated by 40 m for the earlier terrace (Gelasian), about 20 m for the Middle Pleistocene terraces, and between 1,5 and 6 m for the latest (Tyrrhenian). This value is less than the previous estimation [12].

The second limit corresponds to the fault which edges the Nice Range (SBAN Fault., Fig.1), separating it from the Pliocene Basin. The Pliocene molassic layers are bent or even overlapped. The faulting was essentially a dextral strike slip [28] with some additional vertical movement, that of the uplift Alpine Range. The throw is highlighted on the slikensides located on the southern part of the fault, in Nice-city, on the left bank of Paillon River, very close to the present coast [8].

The area on the eastern coast of Nice uplifted from 2 to 7 m (table 3) related to the adjacent sector between the mouth of the River Var and the border of the Alpine range. This uplift may be due to the vertical activity of the Saint-Blaise-Aspremont-Nice fault since MIS 5.5. Other more or less transverse faults which reached the coast, especially the big strike-slip BSM Fault, probably created a favourable context for the offsetting of coastal blocks during the Late Quaternary Age. The uplift of the coast seems to be extend east, as showed by difference of Tyrrhenian sea-level heigh from Puits Risso site to Prince's Cave (Fig.1).

VII. Conclusion.

Owing to recent improvements in U-series analysis (MC-ICP-MS technique), gastropod shells recovered from a Quaternary terrace in Nice were measured in order to date the emplacement of this formation. Results are consistent with a Tyrrhenian age, in full agreement with the morphostratigraphic regional data.

The uplift of the Tyrrhenian marine terrace eastward, observed a long time ago [6], has now been identified on a sufficiently long sector to have been considered to be uninterrupted. On each outcrop, the restoration of the marine level, taking into account the altimetry of the main sedimentary facies encountered on the present beaches profiles, allows us to obtain a satisfactory precision.

The uplift gained eastward : perhaps it is the superficial effect of the Tanneron-Argentera ridge [33]. The uplift is continuous, but two bounds occur crossing known faults : 1/ « the Var Fault » under the present valley and 2/ the western border-fault of the Nice range (Saint-Blaise- Aspremont –Nice Fault). We have noted that the difference in level on both sides of the Var Fault is almost as significant as the one which appears with the border fault crossing of the Nice Range. This result is surprising, taking into account volume and the forces implemented in the arc of Nice and considering that its uplift is about 800 m during

the Late Pliocene [21]. During the Quaternary, its absolute vertical uplift appears rather weak and the SBAN faulting strongly decreases when the differential movement of the Var Fault increases. This latter which probably follows inherited normal faults, has a relatively significant vertical component even in a very moderate compressive context [15].

Involved structures	Uplift in meters maxi mini	Annual rate in mm
Var Fault	(15-9) to (13-11,5)	0,048-0,012
Western border fault of the Nice range (SBAN Fault)	(20-13) to (17-15)	0,056 – 0,016

Table 3 – Uplift rate calculated since the M.I.S. 5.5 (125 k.ans)

With the new U/TH dating, the neotectonic activity during the Late Pleistocene, and the present seismicity are confirmed in this sectors.

References

[1] P. Ambert, M. Ambert, Altitude des lignes de rivage de l'Eutyrrhénien entre Alpes et Pyrénées. Conséquence néotectoniques. Revue d'analyse spatiale quantitative et appliquée, 38 et 39 (1996) 1-20.
[2] E.J. Anthony, M. Dubar, O. Cohen, Les cordons de galets de la Baie des Anges; histoire environnementale et stratigraphique; évolution morphodynamique récente en réponse à des aménagements. Géomorphologie : relief, processus, environnement 2 (1998), 167-188.
[3] L. Barral, S. Simone– La grotte du Prince ; le Pléistocène moyen in : Sites Paléolithiques de la région de Nice et grottes de Grimaldi sous la dir. de Lumley H. et Barral Louis. Livret-guide de l'excursion B1 de l'UISPP, Nice, 1 (1976) 113-122
[4] N. Béthoux, M. Cattaneo, P.Y. Delpech, C. Eva, J.P. Rehault.- Mécanismes au foyer de séismes en mer Ligure et dans le Sud des Alpes Occidentales : résultats et interprétations, C. R. Acad. Sci. Paris., 307, 2 (1988) 71-77.
[5] F. Bigot-Cormier, F. Sage , M. Sosson, J. Deverchère, M. Ferrandini, P. Guennoc, M. Popoff, J.-F. Stéphan, Déformations pliocènes de la marge nord-ligure (France) : les conséquences d'un chevauchement crustal sud-alpin. Bull. Soc. Géol. Fr., 175, 2, (2004) 197-211
[6] E.Bonifay, Le Quaternaire littoral et sous-marin des côtes françaises de la Méditerranée. Etudes françaises sur le quaternaire, VIIe congr. Internat ; INQUA, Paris, 1969, p. 43-55
[7] J. Bourcart et M. Siffre, Le Quaternaire marin du pays niçois. Bull. Soc. Géol. Fr., 21, 1958, 715-730.

[8] J. Cataliotti-Valdina, J.M. Guérin et G. Iaworsky, Une solution au problème de la néotectonique quaternaire dans les Alpes-Maritimes, la part de la tectonique salifère. Bull. Mus. Anthrop. Préhistor. Monaco, 24, 1980, 5-12.
[9] C. Causse, B.Ghaleb, N. Chkir, K. Zouari, H. Ben Ouedzou , A. Mamou, Humidity changes in southern Tunisia during the Late Pleistocene inferred from U-Th dating of mollusc shells. Applied Geochemistry, 18, (2003) 1691-1703.
[10] G. Dardeau (+),M. Dubar, N. Toutin-Morin (+), G.Crévola, C. Mangan, Carte géologique de la France au 1/50 000. Feuille de Grasse-Cannes et Notice (sous presse) BRGM, Orléans.
[11] M. Dubar, Nouvelles données paléoclimatiques sur le Tyrrhénien des Alpes-Maritimes (France). Bull. Ass. Fr. Et. Quat., 25-26, 1986, 63-69
[12] M. Dubar, Y. Guglielmi, Morphogenèse et mouvements verticaux quaternaires en bordure de l'arc de Nice; essai de quantification. Analyse Spatiale et Appliquée, 38 et 39, 1997, 21-27.
[13] M. Dubar, J. L. Perez, Néotectonique quaternaire en bordure de l'arc subalpin de Nice. C. R. Acad. Sci. Paris, 308, II, 1989, 1485-1490.
[14] P.R Federici., M. Pappalardo, Evidence of Marine Isotope stage 5.5 highstand in Liguria (Italy) and its tectonic significance.Quaternary International, 145-146, (2006) 68-77.
[15] Y. Guglielmi, M. Dubar, Analyse morphostructurale du basin pliocène du Var (A.M., France) et confrontation avec les données de la néotectonique. Bull. Inst. Bassin d'Aquitaine, 53, 1993, 77-83.
[16] G.M. Henderson , R.F. Anderson – The U-series toolbox for paleoceanography. Reviews in Mineralogy and Geochemistry, 52, 2003, 493-531.
[17] C. Hillaire-Marcel, C. Gariépy, B. Ghaleb, J-L. Goy, C. Zazo, J. Cuerda Barcelo– U-series measurements in Tyrrhenian deposits from Mallorca – Further evidence for two last-interglacial high sea levels in the Balearic islands. Quaternary Science Reviews, 15,1996, 53-62.
[18] C. Innocent - The quarternary evolution of a kaolonitic weathering profile at Yaou (French Guiana), as investigated by U-series. Abstr. 43th Annual Meeting Clay Mineral Society, Oléron, France , 2006
[19] C. Innocent, C. Bollinger, F. Chabaux, C. Claude, N. Durand, A. Le Faouder, B. Kiefel, C. Pomies - Intercomparison of new Th isotopic standards : Preliminary results. Abs. 14th Goldschmidt Conference, 2004, Copenhague.
[20] C. Innocent, C. Fléhoc, F. Lemeille - U-Th vs. AMS ^{14}C dating of shells from the Achenheim loess (Rhine Graben). Bulletin de la Société Géologique de France, 176, 3, 2005 249-255.
[21] F. Irr, Paléoenvironnements et évolution géodynamique néogène et quaternaire de la bnordure nord du bassin méditerranéen occidental. Thèse Sciences, Nice, 1984, 464 p.
[22] A. Kaufman, B. Ghaleb, J.F. Wehmiller, C. Hillaire-Marcel, Uranium concentration and isotope ratio profiles within *Mercenaria* shells : Geochronological implications. Geochimica et Cosmochimica Acta, 60, 1996, 3735-3746.
[23] H. de Lumley (1976), Les lignes de rivage quaternaire de Provence et de la région de Nice, In : La Préhistoire française, I1, pp. 311-332. Editions du CNRS
[24] J.F. Minster, L.P. Ricard, C.J. Allègre, ^{87}Rb-^{87}Sr chronology of enstatite meteorites. Earth and Planetary Science Letters, 44, 1979, 420-440.
[25] W.D. Nestéroff, Recherche sur les sédiments marins actuels de la région d'Antibes. Annales de l'Institut Géographique, 13, 1959, 1-136.
[26] J.K. Osmond, J.P. May, W.F. Tanner, Age of the Cape Kennedy barrier-and-lagoon complex. Journal of Geophysical Research, 75, 2, 1970, 469-479.
[27] D. Porcelli, P.W. Swarzenski, The behaviour of U- and Th-series nuclides in groundwater. Reviews in Mineralogy and Geochemistry, 52, 2003, p. 317-361.

[28] J.F. Ritz, Evolution du champ de contrainte dans l'arc de Nice depuis 25 millions d'années. D.E.A, Nice, 1986, 61 p.
[29] J.N. Rosholt, $^{230}Th/^{234}U$ dating of travertine and caliche rinds. GSA Abstr. Prog., 8, 1976, 1076.
[30] L. Sage, La sédimentation à l'embouchure d'un fleuve côtier méditerranéen : le Var (A.M.) Thèse de doctorat de spécialité de Géologie, Nice, 1976, 250 p.
[31] F. Sirocko, K. Seelos, K. Schaber, B. Rein, F. Dreher, M. Diehl, R. Lehne, K. Jäger, M Krbetschek., D. Degering, A late Eemian aridity pulse in central Europe during the last glacial inception. Nature, 436, 2005, 833-836.
[32] C.E. Stearns, D.L. Thuber, Th 230- U234 dates of late Pleistocene marine fossils from the Meditrerranean and Marocco. Quaternaria, 7, 1965, 29-42.
[33] J. Vernet, La phase d'édification post-miocène des alpes sur la transversale des Alpes-Maritimes. Bull. Soc. Hist. Nat. Toulouse, 118, 1982, 223-234
[34] G.J. Wasserburg, S.B. Jacobsen, D.J. De Paolo, M.T. Mc Culloch, T.Wen, Precise determination of Sm/Nd ratios, samarium, and neodymium isotopic abundances in standard solutions. Geochimica et Cosmochimica Acta 45, 1981, 2311-2323.
[35] C. Zazo, J.L.Goy, C.J. Dabrio, T. Bardaji, L. Somoza, P.G. Silva, The Last Interglacial in the Mediterranean as a model for the present interglacial, Global and Planetary Change, 7, 1993, 109-117